

TREATMENT OF DIFFRACTION EFFECTS CAUSED BY MOUNTAIN RIDGES

*Rainer Klostius, Andreas Wieser, Fritz K. Brunner
Institute of Engineering Geodesy and Measurement Systems,
Graz University of Technology, Steyrergasse 30, A-8010 Graz, Austria.
E-mail: {rainer.klostius, andreas.wieser, fritz.brunner} @TUGraz.at*

Abstract

A major problem of using GPS for deformation monitoring is signal distortion caused by the objects which form the skyline. Both local obstacles, like trees surrounding the station, and far away obstacles, like mountain ridges, lead to diffraction of the signal. In this paper we show data with corresponding biases in the observations up to 7 cm and a C/N_0 reduction of 10-12 dB.

We discuss three different approaches to mitigate such errors. First we discuss the usage of a constant high cut-off angle when collecting or processing the observations. Alternatively, we investigate the usage of an azimuth-dependent elevation mask to cut out the affected observations. In the third approach, we discuss the mitigation of the effect using different variance models.

The results show that a sufficiently high constant cut-off angle avoids diffraction effects at the obstacles, but the resulting bad geometry significantly reduces the attainable accuracy. The mitigation of the effects can either be reached by an appropriate azimuth-dependent elevation mask, or by using a variance model based on the signal-to-noise ratio, i.e. the SIGMA- ϵ variance model.

1. Introduction

In engineering geodesy, deformation measurement using GPS is a common technique, e.g. for the monitoring of landslides or buildings. Obstacles between the receiver and the satellite may degrade the signal quality and therefore the results. Often these obstacles affect mainly low elevation satellite data, but in an alpine environment, trees or mountain ridges may cause problems also at higher elevation angles. With static applications and long site occupation times, this may still not be a problem, because of the inherent long averaging time. For monitoring applications with kinematic processing or averaging over short times, the impact of diffraction may not be negligible.

The easiest way to eliminate a possible degradation of the signals is to use a sufficiently high elevation cut-off angle, higher than all obstructions. The observations possibly affected by the obstacles are then not used to compute the solution and thus cannot degrade the quality of the results. However, this approach may also reject many good observations, and it degrades the geometry of the solution. Instead, an optimum elevation mask could be derived from the physical horizon, possibly with a small offset. However, the application of such an azimuth-dependent elevation mask requires the horizon to be mapped in advance.

An alternative for mitigating the effect of such obstacles is to use variance models which reduce the impact of the distorted observations on the results. A standard approach for high precision applications is to work with an elevation dependent model, as it is e.g. implemented in the Bernese GPS-Software [1]. Another approach, the SIGMA- ε variance model developed by Hartinger and Brunner [2], uses the carrier-to-noise density ratio (C/N_0) as an input for computing the variances. Due to the antenna gain pattern, the C/N_0 value depends on the elevation of the arriving signal. However the C/N_0 also reflects actual signal distortions and is thus a more useful discriminator of the signal quality than the elevation alone.

In the next section we briefly review the effect which occurs, when satellites rise and set behind an obstruction. In section 3, the data set and the processing schemes used for the subsequent investigation are presented. Section 4 shows the diffraction effects in the observation and coordinate domain, and demonstrates the impact of selecting an appropriate elevation mask. The analysis also shows that using a proper variance model (SIGMA- ε) is another useful tool to suppress the deteriorating effect of the obstacles on the results, even if no specially matched azimuth-dependent elevation mask can be used.

2. Diffraction effects

When an obstacle interferes with the line-of-sight between the satellite and the receiver, one possible effect is the diffraction of the signals. The diffraction allows the GPS-signals to propagate beyond the horizon and behind obstructions. The received field strength in the receiver decreases rapidly as the satellite moves into a shaded region, but this diffracted field still exists, and has often sufficient strength to allow tracking by the receiver.

Diffraction effects can be explained by Huygen's principle. This principle states, that all points on a wavefront can be seen as point sources, which produce secondary wavelets. These wavelets create a new wavefront. Diffraction occurs when these secondary wavefronts propagate into the shaded region. Diffraction loss arises from the blockage of secondary waves, such that only a portion of the initially available energy is diffracted around an obstacle. Additionally, diffraction leads to an increase of the path length of the signal.

In order to roughly estimate the diffraction loss expected at mountain ridges, we assume that the mountain acts as a knife-edge with which the wavefronts interact, see Figure 1.

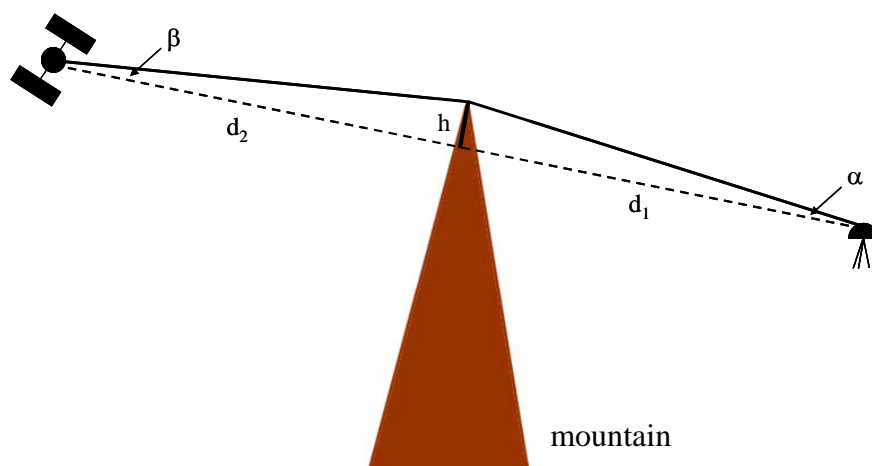


Figure 1: Geometrical representation of the knife-edge effect.

Using equation (17) in [3] and the geometric relations given in Figure 1, we can compute the diffraction loss of the signal. The result is visualized in Figure 2 (a) as a function of the angle α in Figure 1. Assuming a mountainous area, the obstructions occur at an elevation of 15-30°. The C/N_0 of the received signal in such elevations for the used equipment is in the unobstructed case in the range of 45-50 dBHz. In our case the used Ashtech receivers can not track signals lower than 35 dBHz, therefore signals can still be tracked until the loss of signal strength due to obstructions exceeds about 15 dBHz. From Figure 2 (a) follows that satellites will be tracked until they are, for example 0.3° below the mountain ridge in a distance d_1 of 5 km away from the receiver, which is a typical distance for the dataset chosen below.

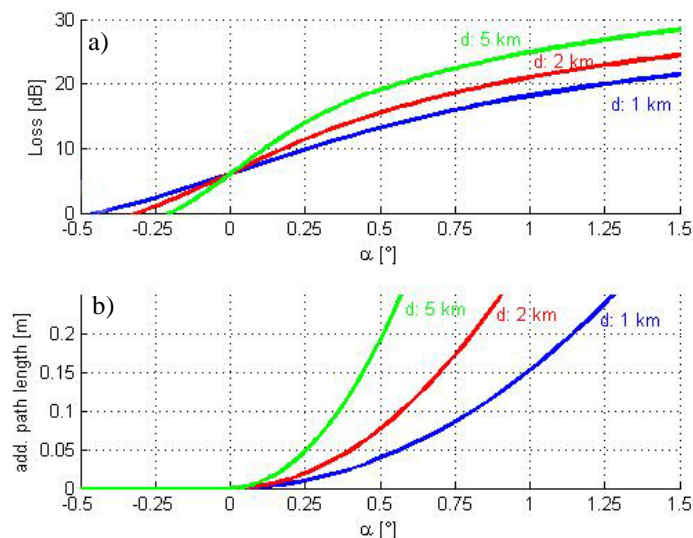


Figure 2: Diffraction loss (a) and additional path length (b) of the signal for distances of 1, 2 and 5 km from the receiver to the obstruction.

From Figure 1 we can also estimate the additional path length caused by diffraction. The result is shown in Figure 2 (b), again as a function of α . Using the above tracking threshold in terms of α (0.3°), we find that the maximum additional path length i.e., the maximum bias of the carrier-phase observable, due to diffraction by the mountain ridge will be approximately 70 mm.

3. Data processing

To visualize the diffraction effects and the possible consequences on the coordinate results, data of a GPS campaign are investigated. The campaign was measured at the Gradenbach landslide located in the northwest of Carinthia, cf. [4]. For this investigation, one 24 hour data set (Dec 12th 2005 12:00 UT to Dec 13th 2005 12:00 UT) for the baseline from reference point R2 to monitoring point MB, was chosen arbitrarily. Table 1 summarizes key parameters of this data set. The obstruction situation in terms of azimuth and elevation of the physical horizon on the two points was measured using a theodolite. Figure 3 gives an impression of the situation at both sites. The distribution of signal strengths (high C/N_0 at high elevation, low C/N_0 at low elevation) is mainly caused by the antenna gain pattern. We note that the mountain ridges cause a rather sharp cut-off of the GPS-signals. The trees do not cause such a sharp cut-off (see separate mask at MB). A detailed investigation also shows a difference between rising and setting satellites. The signal acquisition threshold is usually higher than the signal tracking threshold in a receiver, meaning that the signals have to be stronger for acquisition. Consequently, satellites may be first tracked at higher elevations than when they

set. Due to a lack of time only the combined obstruction mask was obtained at the station R2. The following investigation thus concentrates on signals which are affected by the obstructions at MB, because of the possibility to distinguish between trees and mountain, there.

Table 1: Outline of Gradenbach data sets chosen for this investigation; scale parameters used subsequently with identical-variance model (ID), elevation dependent variance model (ELE), and SIGMA- ϵ variance model (EPS); coordinate random walk spectral noise density (Q) for each of North, East, and Height.

Reference	Antenna	Ashtech Chokering
	Receiver	Ashtech Z-Xtreme
Rover	Antenna	Ashtech Chokering
	Receiver	Ashtech Z-Xtreme
Sampling rate [s]		3
Elevation cut-off angle [°]		0
Baseline length [km]		3.2
ID: σ [mm]		5.6
ELE: σ_0 [mm]		1.4
EPS: C [m ² Hz]		1.21
Q [m ² Hz]		0.01

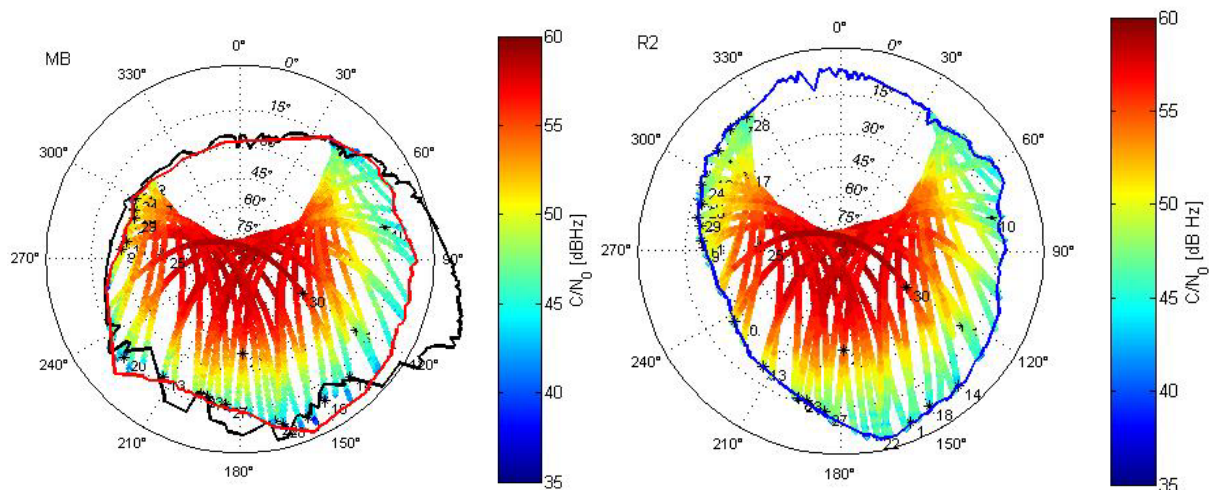


Figure 3: Satellite tracks with measured C/N_0 values at stations MB (left) and R2 (right); obstruction masks on MB: mountains (red), trees (black); combined obstruction mask on R2 (blue).

For this data set, the investigation of the effects in the observation domain was carried out using double-differenced (DD) 'observed-minus-computed' (OC) values:

$$OC = \nabla\Delta\Phi - (\nabla\Delta\rho + \nabla\Delta I + \nabla\Delta T + \nabla\Delta\delta^s \cdot c + \nabla\Delta PCV + \nabla\Delta N) \quad (1)$$

$\nabla\Delta\Phi$... DD observed phase (m)
$\nabla\Delta\rho$... DD geometrical range, incl. antenna offset and relativistic corrections (m)
$\nabla\Delta T$... DD tropospheric correction (m)
$\nabla\Delta I$... DD ionospheric correction (m)
$\nabla\Delta\delta^s$... DD satellite clock error (s)
c	... speed of light in vacuum (m/s)
$\nabla\Delta PCV$... DD phase centre variations (m)
$\nabla\Delta N$... DD initial carrier-phase ambiguity

The OC values were computed using a Kalman Filter MATLAB-package developed at the Institute of Engineering Geodesy and Measurement Systems. As input parameters precise IGS orbits, the Saastamoinen tropospheric model and the Klobuchar ionospheric model were used. The phase centre eccentricities and variations of the used antennas were taken into account using the NGS antenna calibration results which are available on the internet¹. The station coordinates were assumed constant during the 24 hour session, and were taken from previous static processing of the same data using the Bernese GPS-software. Due to the short baseline length in this campaign (see Table 1), we may assume that most of the effects due to ionosphere and troposphere are eliminated by double-differencing and application of the above models. Furthermore, we know that there was no significant motion during the selected session time, so the patterns found subsequently in the OC time series and the coordinate time series are caused by noise and propagation effects like diffraction and multipath.

For the analysis in the coordinate domain, the coordinates of the respective reference point were fixed and those of the rover point were estimated as coordinate random walk using the Kalman Filter program of the above mentioned MATLAB-package. The spectral noise density Q (see Table 1) was deliberately set much higher than the expected motion of the points would require. This allows the estimated coordinates to vary as indicated by the observations and thus show the real impact of distorted observations. It has to be mentioned, that a quality control kernel which performs outlier detection and mitigation is an integral part of the Kalman Filter package and was used during calculation of the coordinate time series.

For the analysis of the effects in the observation domain, OC values computed by the same Kalman Filter program were used (because the ambiguities have to be fixed), but the coordinates of the rover stations were constrained to their initial (true) values. So the OC values represent the error patterns except during periods (few epochs only) with float ambiguities, which may absorb parts of the pattern.

Three different variance models were used: a variance model assuming identical variance of all observations (ID), an elevation dependent model (ELE), and the SIGMA- ε variance model (EPS) [2]. The ELE yields variances

$$\sigma_{ELE}^2 = \frac{\sigma_0^2}{\sin^2(\varepsilon)}, \quad (2)$$

¹ <http://www.ngs.noaa.gov/ANTCAL/>

